

Article

Optimizing Metallographic Etchants for Ancient Gold and Silver Materials

Shengyu Liu ¹, Zisang Gong ¹ , Haizi Lu ², Wei Zhang ³, Yanru Ma ⁴, Xiaolin Yang ⁴, Zhenda Xie ⁵, Gang Hu ^{1,*} and Dongbo Hu ^{1,*}

¹ The International Center for Chinese Heritage and Archaeology, School of Archaeology and Museology, Peking University, Beijing 100871, China; liushengyu@pku.edu.cn (S.L.); gzs98@pku.edu.cn (Z.G.)

² The Sichuan Provincial Cultural Relics and Archaeology Research Institute, Chengdu 610072, China; luhaizi@126.com

³ The Gansu Provincial Cultural Relics and Archaeology Research Institute, Lanzhou 730000, China; m13919106666@163.com

⁴ The National Museum of China, Beijing 100005, China; nmcmyr@icloud.com (Y.M.); yangxl202107@163.com (X.Y.)

⁵ Institute for Advanced Study, Tsinghua University, Beijing 100084, China; xzd18@mails.tsinghua.edu.cn

* Correspondence: hugang@pku.edu.cn (G.H.); hudongbo@pku.edu.cn (D.H.)

Abstract: In recent years, with the excavation of an increasing amount of gold and silver artifacts, there has been an urgent need to optimize the formulations and methods of metallographic etching. Herein, a kinetic control study is performed to investigate the mechanisms leading to poor results when etching ancient gold materials with aqua regia, i.e., when secondary AgCl impurities form during the etching of the sample surface. To this end, a concentrated ammonia and sodium thiosulfate solution is used to dissolve AgCl impurities and obtain high-quality metallographic images of ancient gold materials using a coordination reaction to generate stable free-state coordination ions from Ag⁺. On this basis, a ferric chloride + sodium thiosulfate method is proposed to optimize the formulation of the etchant for ancient silver materials. The formulation is efficient, safe and easy to handle, and solves the problems of the easy failure of the commonly used etchant of ammonia + hydrogen peroxide and the complicated preparation process of acidified potassium dichromate while maintaining the long-term stability of the etched Ag–Cu alloy samples.

Keywords: metallographic research; ancient gold and silver materials; etchants; kinetic control study; silver chloride impurities; coordination reaction



Citation: Liu, S.; Gong, Z.; Lu, H.; Zhang, W.; Ma, Y.; Yang, X.; Xie, Z.; Hu, G.; Hu, D. Optimizing Metallographic Etchants for Ancient Gold and Silver Materials. *Metals* **2022**, *12*, 1229. <https://doi.org/10.3390/met12071229>

Academic Editor: Sebastian Feliú, Jr.

Received: 4 June 2022

Accepted: 18 July 2022

Published: 20 July 2022

Publisher's Note: MDPI stays neutral with regard to jurisdictional claims in published maps and institutional affiliations.



Copyright: © 2022 by the authors. Licensee MDPI, Basel, Switzerland. This article is an open access article distributed under the terms and conditions of the Creative Commons Attribution (CC BY) license (<https://creativecommons.org/licenses/by/4.0/>).

1. Introduction

Metallographic research on archaeological metal artifacts has been performed for over 100 years [1–3]. Metallographic observation is the most direct and effective method to study the development of the smelting, casting and manufacturing processes of ancient metal materials [4]. It is a destructive material testing method that requires the sample to be embedded in an epoxy resin (or phenolic resin) block, pre-ground, and polished to obtain a smooth surface. The polished metal surface does not reveal the details of the microstructure. To observe the grain boundaries, the composition of the different phases, inclusions and other micro traces of the manufacturing process, the polished metal surface must be etched with a suitable chemical reagent (etchant) to reveal the differences in grain orientation and microstructure, and the results are observed and recorded in conjunction with a metallographic microscope (optical microscope) or a scanning electron microscope [5].

The mechanism of etching utilizes the differences in dissolution rates between the different structures and components of the alloys in the specific etchant to show the difference in dissolution morphology [4,6,7], such as grain and grain boundaries, X-enriched

phases and Y-enriched phases (X and Y represent different metal components in the alloy), and metal matrix and intracrystalline particles. Therefore, the suitable etchant for each alloy type is different. In addition, the poor state of preservation of ancient metal materials due to their long-term burial and erosion by groundwater, soil ions, microorganisms, etc., which might result in faster dissolution rates, requires the researcher to adapt the etchant or etching method to the actual condition of the samples to be tested and the metallographic information of interest.

In the case of metal artifacts such as iron and bronze, which have been studied in many samples, there are now well-established, comprehensive and targeted etchants formulations and etching methods to obtain high-quality metallographic images. **Iron:** For this metal, 2–3 vol.% Nital (alcoholic nitric acid) [4,8–10] and 2–3 vol.% methanolic nitric acid [11–13] are the most common etchants and are used in a wide range of applications. In addition, Heyn's reagent (aqueous $\text{CuCl}(\text{NH}_4)$) [10,14], Klemm's reagent (aqueous $\text{Na}_2\text{S}_2\text{O}_3 + \text{K}_2\text{S}_2\text{O}_5$) [4,10,14], Picral (alcoholic $\text{C}_6\text{H}_2(\text{OH})(\text{NO}_2)_3$) and other reagents are used to observe specific grain orientations, microstructures, inclusions and other types of conditions in iron. **Bronze:** Aqueous ferric chloride [15,16] and alcoholic ferric chloride [17–19] are used in extremely wide applications for almost all copper alloys, in addition to saturated solutions of chromium (VI) oxides (CrO_3) and 5% potassium ferricyanide for grain boundary etching and inclusion identification, respectively [4].

However, in the case of gold and silver, due to the relatively small number of excavated artifacts and a limited number of samples, the common etchants are quite simple. **Gold:** The commonly used etchant is aqua regia (a mixture of concentrated hydrochloric acid and concentrated nitric acid) [20–24], sometimes with a small amount of chromium (VI) oxides [25,26] or glycerol [27] to make the grain boundaries clearer; ammonium persulfate + potassium cyanide is occasionally used [20]. **Silver:** Ammonia + hydrogen peroxide [28–30] and acidified potassium dichromate [30–34] are the most common. As a result, researchers often report problems when using these etchants in practice.

- (a) **Gold-aqua regia:** The problem of poorly defined metallographic images and blurred grain boundaries often occurs (Figure S1a). Some researchers have suggested that this phenomenon is caused by over-etching or impurities on the surface of the sample and have responded by properly polishing the sample after etching. However, this treatment may result in new secondary scratches (Figure S1b) and relies on the researchers' personal experience of the experimental procedure, which is not suitable for application;
- (b) **Gold/silver-ammonium persulfate + potassium cyanide:** Although this etchant is suitable for precious metal alloys such as platinum, gold and silver [20], KCN is a highly toxic chemical and may pose a potential health risk to the researcher;
- (c) **Silver-ammonia + hydrogen peroxide:** The oxidation–reduction reaction between two components of this etchant forms N_2 , which leads to failure (in fact, the etchant is usually only effective for approximately 10 min) and can cause considerable inconvenience when many samples must be etched (Figure S1c). Additionally, when using this etchant many bubbles are formed, creating “hollow drums” on the surface of the sample and preventing the etchant from continuously reacting with the metal, which results in unsatisfactory etching results;
- (d) **Silver-acidified potassium dichromate:** The formulation of this etchant is complex and must be diluted in a certain proportion when used. In addition, although the sample is washed after etching, some reagent remains on the surface and creates a slow, continuous dissolution, which can require repolishing the sample after a period of time (this problem also occurs with other etchants).

In recent years, increasing amounts of gold and silver artifacts have been excavated (e.g., the *Sanxingdui site* in Guanghan, Sichuan Province [35]; the *Jiangkou sunken silver site* in Pengzhou, Sichuan Province; the *Tusi Cemetery of the Yang Family* in Zunyi, Guizhou Province [36]; *Murong Zhi tomb of the Tuyu Hun royal Family* in Wuwei, Gansu Province [37], etc.), and there is an urgent need to optimize etchants to improve the experimental efficiency

of metallographic research. In this paper, we explore the mechanism leading to the poor effect of aqua regia for etching ancient gold materials through scientific analysis and simulated etching experiments. Then, we improve the etching method in a targeted manner. On this basis, we optimize the formulation of the etchant for silver artifacts to achieve an easily accessible, simple, safe and stable performance.

2. Materials and Methods

2.1. Chemicals and Materials

Hydrochloric acid (HCl, 36–38%) and nitric acid (HNO₃, 65–68%) were purchased as guaranteed reagents from Xilong Scientific Co., Ltd., Shantou, China. Ammonium hydroxide solution (concentrated ammonia, NH₄OH, 25–28%) was purchased as an analytical reagent from Shanghai Greagent Technology Co., Ltd., Shanghai, China. Hydrogen peroxide solution (H₂O₂, 30%) was purchased as an analytical reagent from Beijing Tongguang Fine Chemicals Co., Ltd., Beijing, China. Sodium thiosulfate (Na₂S₂O₃) was purchased as a guaranteed reagent from Tianjin Yongda Chemistry Co., Ltd., Tianjin, China. Iron (III) chloride (FeCl₃·6H₂O) was purchased as an analytical reagent from Shanghai Hushi Laboratory Equipment Co., Ltd., Shanghai, China.

Epoxy resin was purchased from Guangzhou Shunyicheng Technology Co., Ltd., Guangzhou, China. Water-soluble polishing paste (the particle size, $W = 1, 0.5$) was purchased from Shanghai Naibo Testing Technology Co., Ltd., Shanghai, China. Deionized (DI) water with a specific resistance of 18.25 MΩ·cm was used in all of our experiments.

2.2. Metallographic Observation

The ancient gold/silver samples were embedded in epoxy resin, polished with SiC papers ($P = 400, 800, 1200, 2000$) and finished with water-soluble diamond paste ($W = 1, 0.5$). Then, the polished samples were etched with the appropriate etchants. The metallographic images were taken by a Shangguang 13XF-PC metallographic microscope.

2.3. SEM–EDS Analysis

SEM–EDS analysis was performed by a Hitachi TM3030 scanning electron microscope and BRUKER energy dispersive X-ray spectroscopy (15.00 kV, low vacuum, 90~120 s).

3. Results and Discussion

3.1. Kinetic Control Study of Etching Ancient Gold Materials with Aqua Regia

The ancient gold sample in our study was a detached fragment from a gold artifact (Figure S2a) excavated from the *Sanxingdui site* [35]. The EDS result showed that the composition (wt.%, same as below) of this sample was Au 85.43%–Ag 14.57% (Figure S2b), which indicates that the material was a Au–Ag alloy.

Considering the potential for both excessive dissolution and impurities on the surface of the sample when directly etched with aqua regia, which can cause the problem of poorly defined metallographic images and blurred grain boundaries, diluted aqua regia was used to obtain a controlled etching process to exclude the possibility of excessive dissolution. The etchant was diluted at a ratio of 1:2.5 (6 mL HCl + 2 mL HNO₃ diluted to 20 mL), added dropwise to the polished sample surface, placed under the metallographic microscope, and images were taken and recorded at 20 s intervals (Figure 1). The gradual presence of isometric grains and annealing twins enabled us to interrupt the etching process at any necessary time to achieve control. When the etching process progressed to approximately 100 s, the sample was removed, washed in flowing distilled water, and dried.

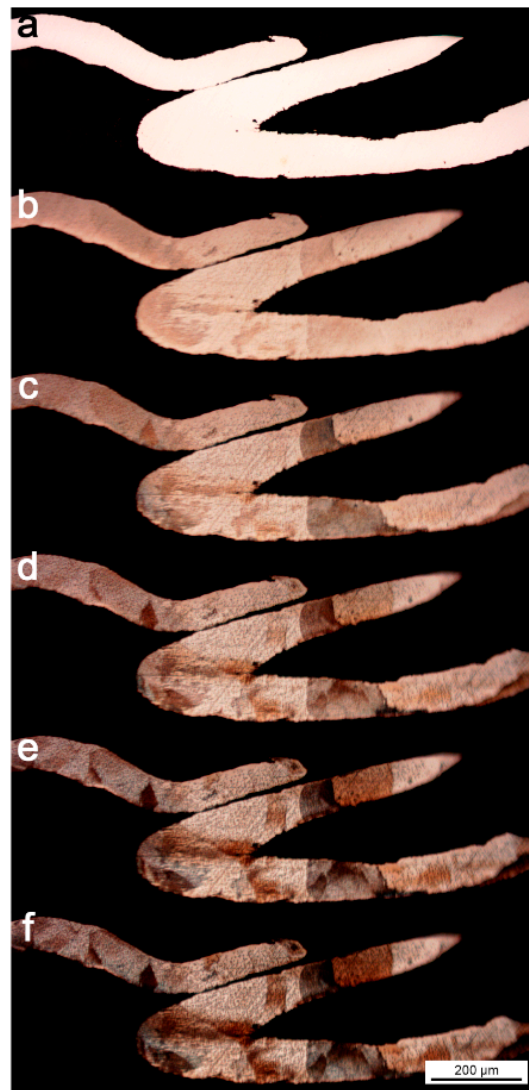
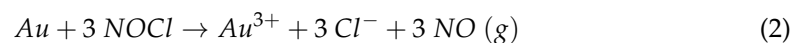
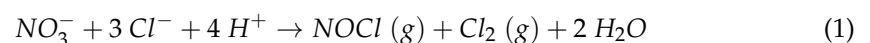


Figure 1. The ancient gold sample (of the gold artifact from the Sanxingdui site) was etched by diluted aqua regia (6 mL HCl + 2 mL HNO₃ and diluted to 20 mL); (a–f) show the morphology of the sample from etching for 0 s to 100 s, respectively (20 s intervals).

The dried sample surface showed a large quantity of diffusely distributed particulate impurities, which obscured the view, but the grain boundaries and slip lines were quite clear underneath the impurities (Figure 2a). The SEM image showed particulate impurities with regular crystal shapes and a maximum diameter of approximately 2 μm (Figure 2b). The EDS mapping analysis showed that the overall composition of this region was Au 58.11%–Ag 28.61%–Cl 13.28%, with Au mainly distributed in the alloy matrix and Ag and Cl in the particulate impurities. Combining the crystalline form, EDS analysis and chemical properties of the reactants, we can deduce that the impurities produced were AgCl crystals which underwent the following reaction process:



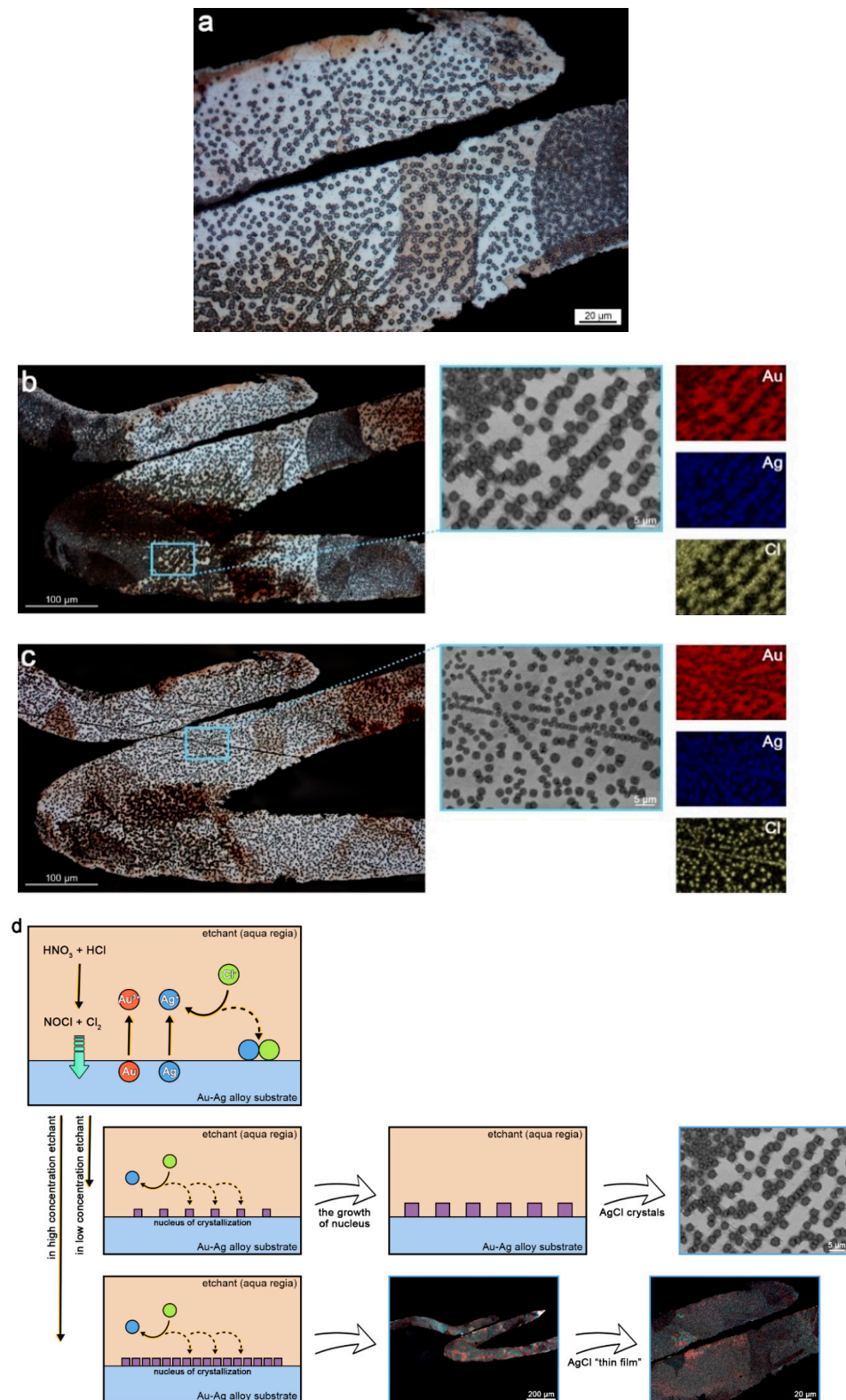


Figure 2. The mechanism of formation of the AgCl impurities. (a) The grain boundaries and slip lines underneath the impurities; (b) SEM image and EDS mapping analysis of the impurities (etchant: 6 mL HCl + 2 mL HNO₃ and diluted to 20 mL; etching duration: 100 s); (c) SEM image and EDS mapping analysis of the impurities (etchant: 6 mL HCl + 2 mL HNO₃ and diluted to 16 mL; etching duration: 40 s); (d) differences in AgCl impurity patterns when using low/high-concentration aqua regia to etch ancient gold samples.

In this case, Equation (1) is the reaction of the two components of aqua regia, HCl and HNO₃ to form nitrosyl chloride (NOCl) and Cl₂, which are responsible for the actual high oxidizing properties of this etchant [38]. Equations (2) and (3) are the processes of dissolution of Au and Ag in the alloy. Equation (4) is the process by which the dissolved Ag⁺ combines with Cl⁻ in the etchant to produce AgCl crystal precipitation.

We verified the reproducibility of this experimental procedure by changing the dilution ratio of the etchant (1:2.0, 6 mL HCl + 2 mL HNO₃ diluted to 16 mL) and the etching time was 40 s. The EDS mapping analysis showed that the region of interest had a composition of Au 65.73%–Ag 27.98%–Cl 6.28%, again with Ag and Cl mainly distributed in the crystals (Figure 2c). The experimental phenomena were similar to those previously described. In addition, we found that the maximum diameter of the precipitated crystals under this condition was relatively small (less than 1.5 μm), possibly due to the short etching time and insufficient growth of the nucleus.

This result reminds us of the crystallography theory that when the concentration of the etchant is low, the rate of Ag dissolution is slow, and only few crystallization nuclei are formed when Ag⁺ combines with Cl⁻. When the etching continues, the nuclei gradually grow, which causes the diffuse distribution of particulate AgCl crystals on the sample surface. At very high concentrations of etchant (pure aqua regia in this paper), the initial dissolution occurred very vigorously, which directly produced many crystallization nuclei densely distributed on the sample surface and formed a structure similar to a AgCl thin film (Figure 2d) [39]. The EDS mapping analysis of the pure aqua regia-etched sample confirmed our idea (Figure S3). High levels of Cl were detected (Au 53.74%–Ag 26.83%–Cl 19.42%), and the distribution was relatively evenly spread over the surface. Thus, we identified the mechanism behind the poor effect of pure aqua regia to etch ancient Au–Ag alloys: the large amount of AgCl impurities was uniformly distributed on the surface of the etched samples and hindered the observation of grain boundaries and metallographic microstructures.

3.2. Removal of Silver Chloride Impurities

Having investigated the mechanism of the poor etching results, we should turn our attention to the removal of the AgCl impurities. AgCl is a cubic crystal system with the closest packing of Cl⁻ in a face-centered cubic structure and Ag⁺ filling the octahedral voids. The solubility product constant (K_{sp}) of AgCl was 1.56×10^{-10} (298 K) [39], which suggests that it would be difficult to remove the secondary AgCl from the sample surface by conventional distilled water washing and drying. Therefore, mechanical or chemical methods were initially considered to study and compare the removal results. For visual comparison, the sample was etched using a 1:2.5 dilution of the etchant (100 s etching time) to obtain a clear volume of particulate AgCl impurities in advance (Figure 3a).

Rubbing is the simplest method of mechanical removal. We attempted to remove AgCl by gently rubbing the etched surface with a skimmed cotton swab dipped in alcohol. The results show that this method could remove AgCl impurities to some extent but might introduce many secondary scratches, which would greatly affect the subsequent observation and judgement of the metallographic organization of the sample (Figure S4). Ultrasonic cleaning is also a common method of mechanical removal. However, the results of the pre-experiments showed that this method had very little success. Moderate polishing of the etched sample may provide better results (Figure S1b), but this method will also introduce secondary scratches and is not suitable for application, as it heavily relies on the personal experimental experience of researchers.

AgCl is normally insoluble in distilled water, but it can be dissolved in a specific solution by using certain ligands to form more stable free state coordination compounds with Ag⁺, which is the basic idea of the chemical removal method. Common Ag⁺ ligands, coordination numbers and accumulative stability constants are shown in Table 1 [40]. The solubility of AgCl in the corresponding ligand solutions can be calculated from the stability constants. The following is an example of ammonia (NH₄OH).

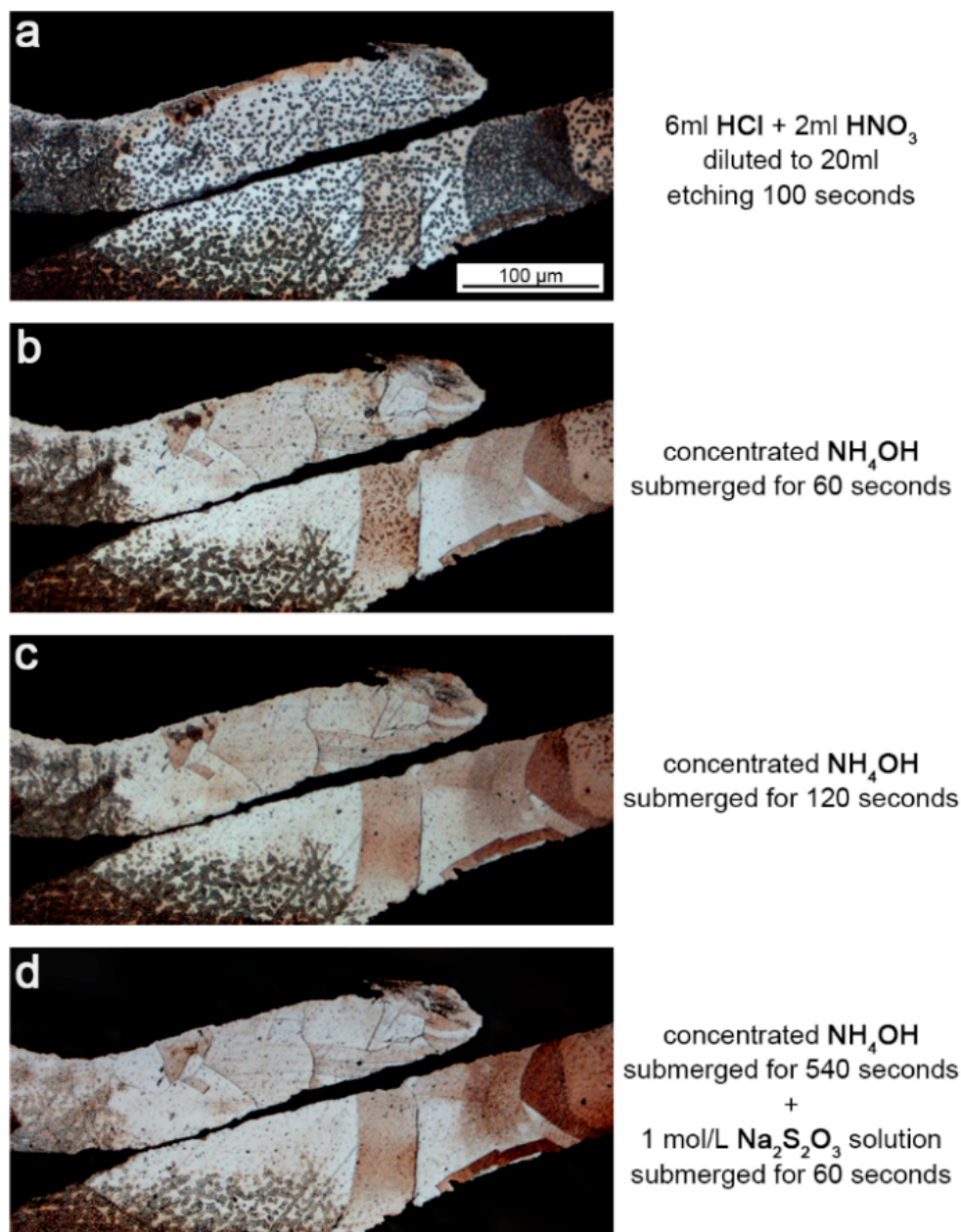
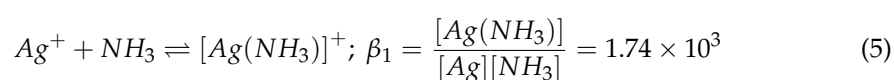


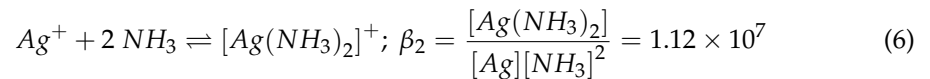
Figure 3. Removal experiment of AgCl impurities. (a) The original sample etched by diluted aqua regia; (b,c) the sample surface after treatment with concentrated ammonia; (d) the sample surface after further treatment with 1 mol/L sodium thiosulfate solution.

Table 1. Common Ag⁺ ligands, coordination numbers, and accumulative stability constants.

Ag ⁺ Ligand (X)	Coordination Number (n)	Accumulative Stability Constant (lgβ _n)
NH ₃	1, 2	3.24, 7.05
S ₂ O ₃ ²⁻	1, 2	8.82, 13.46
CN ⁻	2, 3, 4	21.1, 21.7, 20.6
Br ⁻	1, 2, 3, 4	4.38, 7.33, 8.00, 8.73
SCN ⁻	1, 2, 3, 4	4.6, 7.57, 9.08, 10.08

Ag⁺ has two coordination ion forms with NH₃: [Ag(NH₃)]⁺ and [Ag(NH₃)₂]⁺. In solution:





According to Equations (5) and (6), the distribution of the coordination ions at each level can be obtained:

$$[\text{Ag}(\text{NH}_3)] = [\text{Ag}] \beta_1 [\text{NH}_3]; [\text{Ag}(\text{NH}_3)_2] = [\text{Ag}] \beta_2 [\text{NH}_3]^2$$

We express the total concentration of various forms of Ag-containing ions in the solution as $c_{\text{Ag-NH}_3}$ and the total concentration of various forms of NH_3 -containing ions as c_{NH_3} , as follows:

$$c_{\text{Ag-NH}_3} = [\text{Ag}] + [\text{Ag}(\text{NH}_3)] + [\text{Ag}(\text{NH}_3)_2] = [\text{Ag}](1 + \beta_1 [\text{NH}_3] + \beta_2 [\text{NH}_3]^2) \quad (7)$$

$$\begin{aligned} c_{\text{NH}_3} &= [\text{NH}_3] + [\text{Ag}(\text{NH}_3)] + 2 [\text{Ag}(\text{NH}_3)_2] \\ &= [\text{NH}_3] + [\text{Ag}] \beta_1 [\text{NH}_3] + 2 [\text{Ag}] \beta_2 [\text{NH}_3]^2 \end{aligned} \quad (8)$$

According to the dissolution equilibrium, there is:

$$K_{sp} = [\text{Ag}][\text{Cl}] = 1.56 \times 10^{-10} \quad (9)$$

Since Ag^+ released during the dissolution of AgCl is equal to Cl^- , and there are no other forms of Cl^- -containing ions in solution, $[\text{Cl}] = c_{\text{Ag-NH}_3}$. When the concentration of the ligand solution is 1 mol/L, we have $c_{\text{NH}_3} = 1$ mol/L, $[\text{NH}_3] = 9.23 \times 10^{-1}$ mol/L, and $c_{\text{Ag-NH}_3} = 3.86 \times 10^{-2}$ mol/L. In other words, a maximum of 55.3 mg ($m_{\text{AgCl-NH}_3} = c_{\text{Ag-NH}_3} \times 10 \text{ mL} \times \overline{M}_{\text{AgCl}}$) of AgCl can be dissolved in 10 mL of 1 mol/L ammonia. Similarly (Table S1), when the concentration of other ligand solutions is 1 mol/L, we can calculate that $m_{\text{AgCl-S}_2\text{O}_3^{2-}} = 7.12 \times 10^{-1}$ g, $m_{\text{AgCl-CN}^-} = 7.15 \times 10^{-1}$ g, $m_{\text{AgCl-Br}^-} = 6.78 \times 10^{-6}$ g, and $m_{\text{AgCl-SCN}^-} = 6.62 \times 10^{-6}$ g.

From the calculation results, $\text{S}_2\text{O}_3^{2-}$ and CN^- should be the more effective ligands for dissolving AgCl . However, although ammonia is less capable of dissolving AgCl at 1 mol/L, when concentrated ammonia is used, the theoretical calculation result is $m_{\text{AgCl-NH}_3^*} = 8.53$ g ($c_{\text{NH}_3} \approx 12$ mol/L). Considering the accessibility of reagents and the safety and efficiency of dissolving AgCl , we decided to use concentrated ammonia and 1 mol/L $\text{Na}_2\text{S}_2\text{O}_3$ solution in the dissolution experiments.

The experimental results showed that when the etched ancient Au–Ag alloy sample was immersed in concentrated ammonia, the particulate AgCl crystals on the surface rapidly and more fully dissolved with a longer immersion time (Figure 3b); when the immersion time reached 120 s, the degree of dissolution no longer significantly changed (until 540 s, Figure 3c). At this point, the sample was washed and immersed in 1 mol/L $\text{Na}_2\text{S}_2\text{O}_3$ solution. The AgCl crystals were further dissolved (Figure 3d). These results show that both concentrated ammonia and 1 mol/L $\text{Na}_2\text{S}_2\text{O}_3$ solution positively affect the removal of AgCl impurities, with the latter being slightly effective.

3.3. Optimizing the Etching Methods for Ancient Au–Ag Alloys

Following the idea of aqua regia etching + concentrated ammonia/ $\text{Na}_2\text{S}_2\text{O}_3$ solution for the removal of impurities, we collected a full range of metallographic information on our Au–Ag alloy sample from the *Sanxingdui* site (Figure 4). During our experiment, we adjusted the concentration of the etchant or the length of etching to obtain better quality metallographic images (the specific etching methods are indicated in the notes of Figure 4).

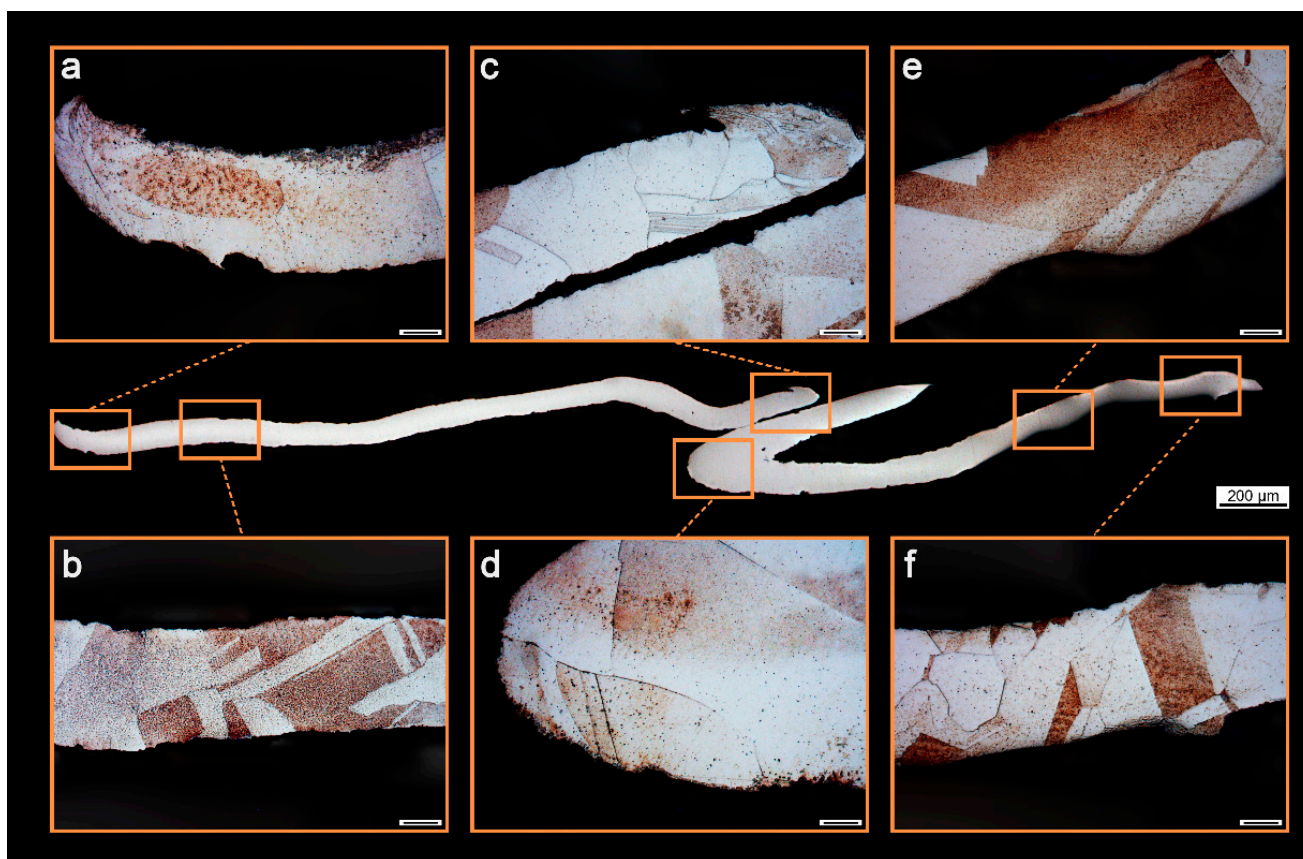


Figure 4. The full range of metallographic information obtained through aqua regia etching + concentrated ammonia/sodium thiosulfate solution removal of impurities (scale bar, 200 μm). (a) Etchant: aqua regia with dilution ratio 1:1.5; etching duration: 40 s; impurity removal: 1 mol/L sodium thiosulfate solution—80 s; (b,e,f) etchant: pure aqua regia; etching duration: 10 s; impurity removal: 1 mol/L sodium thiosulfate solution—80 s; (c) etchant: pure aqua regia; etching duration: 10 s; impurity removal: concentrated ammonia—200 s; (d) etchant: aqua regia with dilution ratio 1:2; etching duration: 50 s; impurity removal: 1 mol/L sodium thiosulfate solution—120 s.

In this process, we utilized the following optimization methods to etch ancient Au–Ag alloys:

- (a) **Rapid etching:** The etchant is pure aqua regia, and the etching time is approximately 10 s. The morphology of the AgCl impurities is a “thin-film” pattern. Both concentrated ammonia and 1 mol/L $\text{Na}_2\text{S}_2\text{O}_3$ solution can be used to efficiently remove AgCl impurities;
- (b) **Local etching:** The etchant is diluted aqua regia, the dilution ratio can be adjusted according to the composition of the Au–Ag alloy samples (1:1.5–1:2.5 ranging), and the length of etching is 30–100 s according to the dilution ratio. The advantage of this method is that the etching process of the region of interest can be observed under the metallographic microscope, and the end point of the etching can be flexibly controlled. The morphology of the AgCl impurities is a “particulate crystal” pattern, which requires a long immersion time with concentrated ammonia or 1 mol/L $\text{Na}_2\text{S}_2\text{O}_3$ solution; thus, ammonia may face the problem of volatilization, and it is better to use $\text{Na}_2\text{S}_2\text{O}_3$ solution.

3.4. Optimizing the Etchant Formulations for Ancient Silver Material

We have found that etchant + secondary AgCl impurity removal solutions are very effective for metallographic studies of ancient gold materials, which we may similarly

introduce into the optimization of etchant formulations for ancient silver materials, giving preference to a chlorine-based etchant + concentrated ammonia/ $\text{Na}_2\text{S}_2\text{O}_3$ solution. As we mentioned earlier, the basic mechanism of etching is to exploit the differences in dissolution rates between different structures and components of the alloy in the specific etchant [4]; in other words, solutions that likely cause the dissolution of various components of ancient silver materials (mainly Ag–Cu alloys) can be used in our experiments.

The first etchant that we should consider is aqua regia. Its strong oxidizing properties cause the dissolution of Au materials, and thus we expected the same result for the Ag–Cu alloys. We used a 1:1.5 dilution of aqua regia to etch the silver sample from a silver bowl (No. G1.2, Ag 96.89%–Cu 3.11%) excavated in Yiwu City (etching time 15 s). Similar to the observed phenomenon after the pure aqua regia etching of the Au–Ag sample (Figure S5a), the EDS results showed that the same AgCl “thin film” was produced during the etching process and covered the surface of the sample (Figure S5b). After treating the AgCl impurities with 1 mol/L $\text{Na}_2\text{S}_2\text{O}_3$ solution, we obtained a metallographic image of excellent quality (Figure 5). Thus, the aqua regia + secondary AgCl impurity removal solution approach worked. However, since the Ag–Cu alloys were much less resistant to dissolution than the Au–Ag alloys, the aqua regia must be diluted in the process of etching the ancient silver materials to avoid reacting too quickly and exceeding the appropriate critical point; similar to the ammonia + hydrogen peroxide etchant system, the diluted aqua regia may face failure, and a higher dilution ratio corresponds to a shorter effective time (during our experiments, the effectiveness of the 1:2.5 dilution of aqua regia did not last more than half an hour), which obviously does not satisfy our experimental needs.



Figure 5. The ancient silver sample (of the silver bowl excavated in Yiwu City) was etched by diluted aqua regia (6 mL HCl + 2 mL HNO_3 and diluted to 12 mL); etching duration: 15 s; impurity removal: 1 mol/L sodium thiosulfate solution for 60 s.

Ferric chloride (FeCl_3) is a common etchant for bronze as it is efficient, safe, and easy to handle. Normally, Fe^{3+} cannot be used to etch ancient silver materials because the standard electrode potential of $\text{Fe}^{3+} \rightarrow \text{Fe}^{2+}$ $\{\varphi^\ominus(\text{Fe}^{3+}/\text{Fe}^{2+}) = 0.771 \text{ V}\}$ is lower than that of silver $\{\varphi^\ominus(\text{Ag}^+/\text{Ag}) = 0.799 \text{ V}\}$. However, in the presence of Cl^- , Cl^- will reduce the silver electrode potential, which may enable the etching of Ag–Cu alloys. We can use a 1 mol/L FeCl_3 solution as an example for theoretical calculations [41].

For the electrode reaction $\text{Ag}^+ \rightarrow \text{Ag}$, according to the Nernst equation:

$$\varphi = \varphi^\ominus + \frac{RT}{F} \lg[\text{Ag}] = \varphi^\ominus + 0.0592 \lg[\text{Ag}] \quad (10)$$

According to Equation (9), $[\text{Ag}] = 5.20 \times 10^{-11} \text{ mol/L}$, which can be calculated and substituted into (10) to obtain $\varphi(\text{AgCl}/\text{Ag}) = 0.191 \text{ V}$. The calculation results show that

$\varphi^{\ominus}(\text{Fe}^{3+}/\text{Fe}^{2+}) > \varphi^{\ominus}(\text{Cu}^{2+}/\text{Cu}) > \varphi(\text{AgCl}/\text{Ag})$, which implies that 1 mol/L FeCl_3 solution can be used to etch Ag–Cu alloys.

The experimental results show that high-quality metallographic images of Ag–Cu alloys can be obtained using the FeCl_3 (etchant) + $\text{Na}_2\text{S}_2\text{O}_3$ (secondary AgCl impurity removal solution) approach (Figure 6a–d). To verify the wide applicability of this method, further experiments were performed on samples of the silver plate (No. G11, Ag 98.08%–Cu 1.93%) and bowl (No. G14, Ag 98.44%–Cu 1.56%) excavated from the *Murong Zhi tomb*, and similarly good results were obtained (Figure 6e,f).

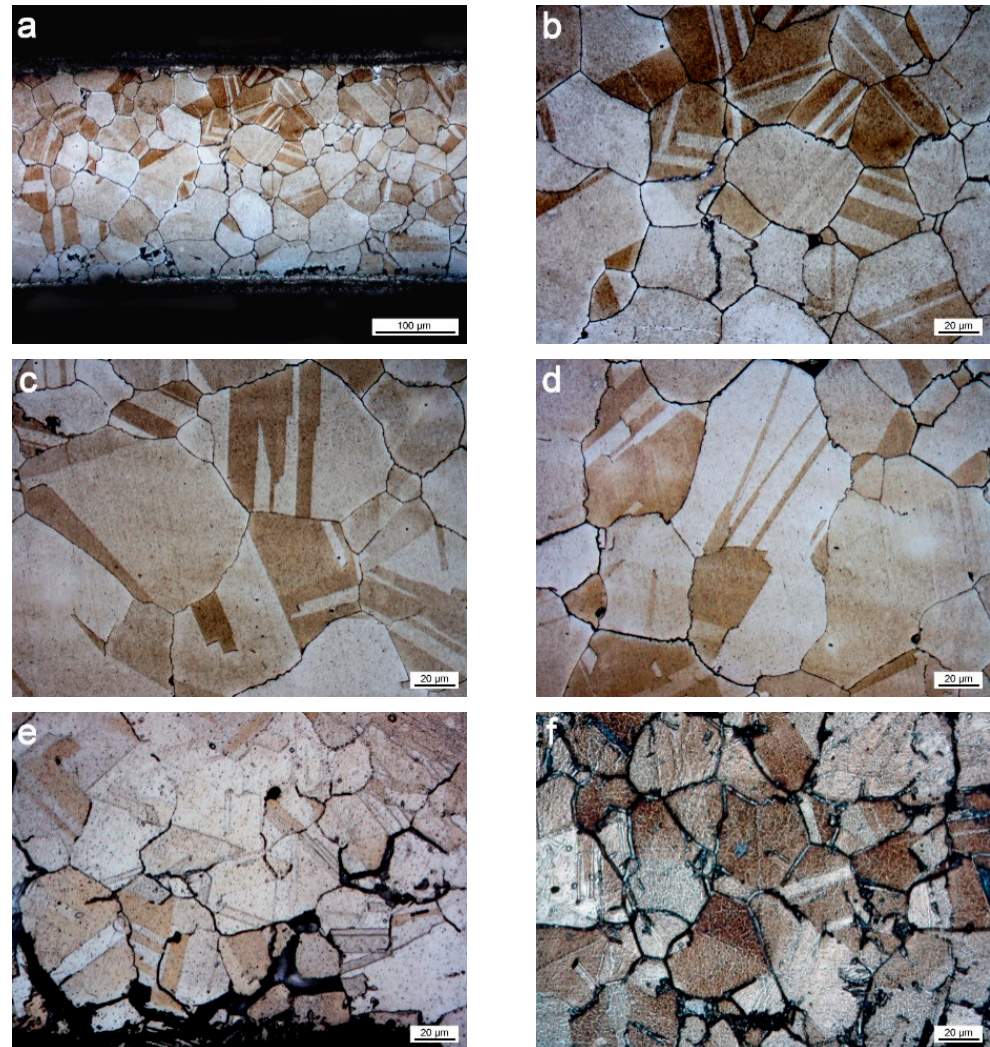


Figure 6. The ancient silver samples were etched by 1 mol/L ferric chloride solution (etching duration: 20 s), and impurities were removed by 1 mol/L sodium thiosulfate solution (for 120 s). (a–d) Ancient silver sample of the silver bowl excavated in Yiwu City; (e,f) ancient silver samples from Murong Zhi tomb.

In addition, we found that the metallographic images of the samples treated by the above approach remained at high quality after a long period of time (over 3 months in this paper, Figure 7a,b) with only a slight increase in color. We acknowledge the possibility that the $\text{Na}_2\text{S}_2\text{O}_3$ solution used to remove the AgCl impurities neutralized the remaining FeCl_3 solution on the surface of the samples. These results indicate that our optimization of the etchant formulation for the ancient silver materials was very successful.

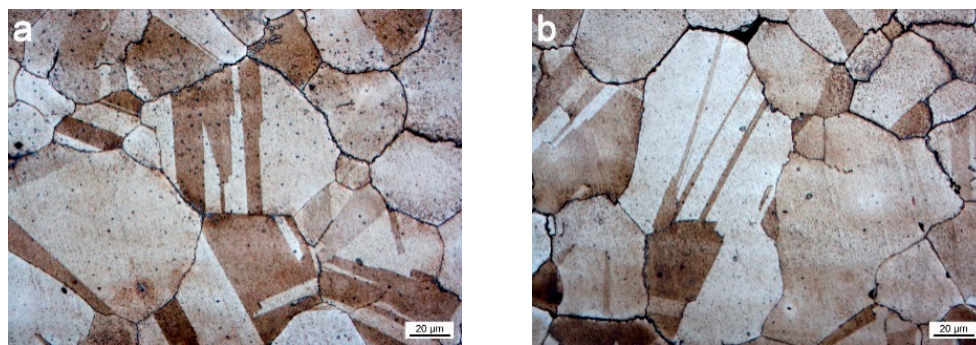


Figure 7. Reobservation of the etched sample after three months. (a) Corresponds to the same region as Figure 6c; (b) corresponds to the same region as Figure 6d.

4. Conclusions

In this paper, we first investigated the mechanism of poorly defined metallographic images and blurred grain boundaries of ancient gold materials etched by aqua regia using a detached fragment from the gold artifact excavated from the *Sanxingdui* site as a sample through controlled simulated etching experiments. The results show that the Ag^+ released from the metal matrix during the etching process reacted with Cl^- in the etchant to form AgCl impurities and covered the sample surface. When pure aqua regia was used, the impurities were in the form of AgCl “thin film”, and when diluted aqua regia was used, they were in the form of “particulate crystals”, both of which obscured the surface morphology of the sample to varying degrees and affected the observation and recording of the metallographic organization.

Subsequently, theoretical calculations and experimental investigations were performed to demonstrate that certain ligands undergo coordination reactions with Ag^+ to generate stable free-state coordination ions that can dissolve the AgCl impurities on the etched sample surface. Both concentrated ammonia and 1 mol/L sodium thiosulfate solution proved to be effective in dissolving AgCl . However, concentrated ammonia was less effective than sodium thiosulfate solution in treating particulate AgCl crystals due to the possibility of volatilization failure.

Finally, we optimized the formulation of etchants for ancient silver materials using chlorine-based etchant + secondary AgCl impurity removal solutions and concluded that a combination of ferric chloride + sodium thiosulfate solution was the better approach. This method is highly efficient, safe and easy to handle, which is lacking in the commonly used etchants for Ag-Cu alloys. This method was applied on silver artifacts excavated from Yiwu City and silver artifacts excavated from *Murong Zhi tomb* with excellent results.

Supplementary Materials: The following supporting information can be downloaded at: <https://www.mdpi.com/article/10.3390/met12071229/s1>. Figure S1: Problems with commonly used ancient gold/silver material etchants; Figure S2: The ancient gold material used in this study; Figure S3: The AgCl “thin film” of the pure aqua regia-etched gold sample; Figure S4: Comparison of the effectiveness of silver chloride impurities rubbed off (scale bar: 20 μm); Figure S5: The AgCl “thin film” of the diluted aqua regia-etched silver sample; Table S1: Calculation process for $\text{m}_{\text{AgCl}_2\text{S}_2\text{O}_3^{2-}}$, $\text{m}_{\text{AgCl}_2\text{CN}^-}$, $\text{m}_{\text{AgCl}_2\text{Br}^-}$ and $\text{m}_{\text{AgCl}_2\text{SCN}^-}$.

Author Contributions: S.L. developed the concept, performed the experiments, and analyzed the experimental data; Z.G., Y.M. and X.Y. contributed to the metallographic experiment; S.L., H.L. and W.Z. prepared the samples; Z.X. designed the program to calculate the m_{AgCl} results; S.L. wrote the manuscript; G.H. and D.H. designed and directed the project. All authors have read and agreed to the published version of the manuscript.

Funding: This research was financially supported by the National Key R&D Program of China (No. 2019YFC1520201).

Institutional Review Board Statement: Not applicable.

Informed Consent Statement: Not applicable.

Data Availability Statement: The dataset supporting the conclusions of this article is included within the article (and its Supplementary Information file).

Acknowledgments: We thank the Sichuan Provincial Cultural Relics and Archaeology Research Institute, the School of Archaeology and Museology, Sichuan University, the School of Cultural Heritage and Information Management, Shanghai University, and the Gansu Provincial Cultural Relics and Archaeology Research Institute for their outstanding support of the samples used in this work.

Conflicts of Interest: The authors declare no conflict of interest.

References

1. Chikashige, M. A Study of ancient Eastern bronze mirrors. *Hist. Rev.* **1918**, *3*, 178–203.
2. Shigeru, K.; Yamauchi, S. Chemical studies of ancient mirrors. *J. Orient. Stud.* **1937**, *8*, 11–31.
3. Yetts, W.P. Problems of Chinese bronzes. *J. R. Cent. Asian Soc.* **1931**, *18*, 399–402. [[CrossRef](#)]
4. Scott, D.A. *Metallography and Microstructure of Ancient and Historic Metals (Translated by Tian, X.; Ma, Q.)*; Chinese Translation Science Press: Beijing, China, 2012; pp. 69–78.
5. Sun, S.; Han, R.; Li, X. *Microstructure Atlas of Ancient Chinese Metallic Materials—Non-Ferrous Metals Volume*; Science Press: Beijing, China, 2011; pp. 25–36.
6. Yu, Y. *Principles of Metallurgy (Upper)*, 3rd ed.; Metallurgical Industry Press: Beijing, China, 2020; pp. 521–533.
7. Yuan, Z.; Dai, Q. *Metallic Materials*, 3rd ed.; Chemical Industry Press: Beijing, China, 2019; pp. 3–17.
8. Cho, N.; Lee, H.; Lee, J. Microstructure and heat treatment of Early Iron Age cast iron axes excavated from the Sinpung site, Wanju, Jeonbuk, in the Korean Peninsula. *Archaeol. Anthropol. Sci.* **2019**, *11*, 2611–2621. [[CrossRef](#)]
9. Ashkenazi, D.; Golan, O.; Tal, O. An archaeometallurgical study of 13th-century arrowheads and bolts from the Crusader Castle of Arsuf/Arsur. *Archaeometry* **2013**, *55*, 235–257. [[CrossRef](#)]
10. Haubner, R.; Strobl, S.; Zbiral, J.; Gusenbauer, C.; Pintz, U. Metallurgical characterization of a coated Roman iron coin by analytical investigations. *Archaeometry* **2016**, *58*, 441–452. [[CrossRef](#)]
11. Park, J.-S.; Rehren, T. Large-scale 2nd to 3rd century AD bloomery iron smelting in Korea. *J. Archaeol. Sci.* **2011**, *38*, 1180–1190. [[CrossRef](#)]
12. Park, J.-S.; Honeychurch, W.; Chunag, A. Iron technology and medieval nomadic communities of East Mongolia. *Archaeol. Anthropol. Sci.* **2019**, *11*, 555–565. [[CrossRef](#)]
13. Gelegdorj, E.; Chunag, A.; Gordon, R.B.; Park, J.-S. Transitions in cast iron technology of the nomads in Mongolia. *J. Archaeol. Sci.* **2007**, *34*, 1187–1196. [[CrossRef](#)]
14. Vander Voort, G.F. *Metallography: Principles and Practice*; ASM International: Novelt, OH, USA, 2004; p. 642.
15. Mödlinger, M.; Trebsche, P. Work on the cutting edge: Metallographic investigation of Late Bronze Age tools in southeastern Lower Austria. *Archaeol. Anthropol. Sci.* **2021**, *13*, 125. [[CrossRef](#)] [[PubMed](#)]
16. Piccardo, P.; Vernet, J.; Voland, G.; Ghiara, G. Metallographic investigation of Early Bronze Age armbands from Western Switzerland (ca. 2200–1500 BC): New highlights about early manufacturing processes. *Archaeol. Anthropol. Sci.* **2020**, *12*, 215. [[CrossRef](#)]
17. Sáenz-Samper, J.; Martínón-Torres, M. Depletion gilding, innovation and life-histories: The changing colours of Nahuange metalwork. *Antiquity* **2017**, *91*, 1253–1267. [[CrossRef](#)]
18. Oudbashi, O.; Hasanpour, A.; Jahanpoor, A.; Rahjoo, Z. Microscopic and microanalytical study on Sasanian metal objects from Western Iran: A case study. *Sci. Technol. Archaeol. Res.* **2017**, *3*, 194–205. [[CrossRef](#)]
19. Oudbashi, O.; Hessari, M. Iron Age tin bronze metallurgy at Marlik, Northern Iran: An analytical investigation. *Archaeol. Anthropol. Sci.* **2017**, *9*, 233–249. [[CrossRef](#)]
20. Scott, D.A. The La Tolita-Tumaco Culture: Master Metalsmiths in Gold and Platinum. *Lat. Am. Antiq.* **2011**, *22*, 65–95. [[CrossRef](#)]
21. Monge Soares, A.M.; Valério, P.; Silva, R.J.C.; Cerqueira Alves, L.; De Fátima Araújo, M. Early Iron Age gold buttons from South-Western Iberian Peninsula. Identification of a gold metallurgical workshop. *Trab. Prehist.* **2010**, *67*, 501–510. [[CrossRef](#)]
22. Liu, X.; Jiang, L.; Zhou, X.; Li, P.; Xiao, L. Protection and restoration of gold and silver inlaid belt hook unearthed from Feihu village, Pujiang County, Chengdu. *Sci. Conserv. Archaeol.* **2021**, *33*, 75–82.
23. Shao, A.; Mei, J.; Chen, K.; Zhou, G.; Wang, H. Preliminary analysis of the metal ornaments unearthed from the Majiayuan Graveyard of the warring states in Zhangjiachuan. *Cult. Relics* **2010**, *10*, 88–96.
24. Wu, H. Analysis on Production Process of Gold Mask Unearthed from Poma Graveyard in Zhaosu County. Master's Thesis, Northwest University, Shaanxi, China, December 2019.
25. Meng, X.; Mei, J.; Dong, Y.; Feng, S.; Han, C. The preliminary analysis of metal tools excavated from tomb M10 from Xiangyang Chenpo burial site in Hubei. *Jiangnan Archaeol.* **2009**, *4*, 106–113.
26. Xie, X.; Li, Y.; Jing, Y.; Wang, X. A preliminary study on some metal objects unearthed from Yihe-Nur M1, Zhengxiangbai Banner, Inner Mongolia. *Steppe Cult. Relics* **2020**, *2*, 110–117.
27. Xiang, X.; Bai, X. Grain refinement of 18-Carat Au-Ag-Cu-Zn alloy containing cerium. *Int. J. Met.* **2015**, *10*, 100–105.

28. Merkel, S.W. Evidence for the widespread use of dry silver ore in the Early Islamic period and its implications for the history of silver metallurgy. *J. Archaeol. Sci.* **2021**, *135*, 105478. [[CrossRef](#)]
29. Northover, P.; Northover, S.; Wilson, A. Microstructures of ancient and historic silver. In Proceedings of the International Council of Museums ICOM-CC, Edinburgh, UK, 16–20 September 2013.
30. Wang, Y. Scientific Study on Decorative Sheetmetal Artifacts Unearthed in the Region of the Chu Culture of the Eastern Zhou Period. Ph.D. Thesis, University of Science and Technology, Beijing, China, December 2019.
31. Mortazavi, M.; Naghavi, S.; Khanjari, R.; Agha-Aligol, D. Metallurgical study on some Sasanian silver coins in Sistan Museum. *Archaeol. Anthropol. Sci.* **2018**, *10*, 1831–1840. [[CrossRef](#)]
32. Shalev, S.; Shechtman, D.; Shilstein, S.S. A study of the composition and microstructure of silver hoards from Tel Beth-Shean, Tel Dor, and Tel Miqne, Israel. *Archaeol. Anthropol. Sci.* **2014**, *6*, 221–225. [[CrossRef](#)]
33. Török, b.; Benke, M.; Mertinger, V.; Barkóczy, P.; Kovács, A.; Hoppál, K.; Kovács, P. Complex metallographic study on Gepid bronze and silver buckles from the Great Hungarian Plain (5–6th cent.). *STAR: Sci. Technol. Archaeol. Res.* **2017**, *3*, 245–252. [[CrossRef](#)]
34. Faieta, R.; Guida, G.; Vidale, M. A preliminary note on the metallography and chemical analysis of silver samples from the Mahboubian Collection, London. *Iran* **2018**, *56*, 144–147. [[CrossRef](#)]
35. Lei, Y.; Li, H.; Yu, M. Gold mask excavated from No.5 pit of the sacrificial area at the Sanxingdui site. *Sichuan Cult. Relics* **2022**, *2*, 107–118.
36. Zhou, B.; Peng, W. Tusi cemetery of the Yang Family at Xinpu Town, Zunyi City, Guizhou Province. *Archaeology* **2015**, *7*, 87–100.
37. Chen, G.; Sha, C.; Liu, B.; Zhang, W.; Wang, S. A brief report on the excavation of the Murong Zhi tomb of the Tuyu Hun royal Family during the early Tang Dynasty in Gansu Province. *Archaeol. Cult. Relics* **2021**, *2*, 15–38.
38. Massucci, M.; Clegg, S.L.; Brimblecombe, P. Equilibrium partial pressures, thermodynamic properties of aqueous and solid phases, and Cl₂ production from aqueous HCl and HNO₃ and their mixtures. *J. Phys. Chem. A* **1999**, *103*, 4209–4226. [[CrossRef](#)]
39. Ye, T. *Principles and Applications of Chemical Crystallization Processes*, 3rd ed.; Beijing University of Technology Press: Beijing, China, 2020; pp. 23–48.
40. Luo, Q. *Coordination Chemistry*; Science Press: Beijing, China, 2012; pp. 135–139.
41. Bard, A.J.; Faulkner, L.R. *Electrochemical Methods—Fundamentals and Applications*, 2nd ed.; Chemical Industry Press: Beijing, China, 2005; pp. 32–38.